Risk assessment of sea ice disasters on fixed jacket platforms in the Liaodong Bay

Ning Xu[1], Shuai Yuan[1], Xueqin Liu[1], Yuxian Ma[1], Wenqi Shi[1], Dayong Zhang [2]

[1]National Marine Environmental Monitoring Centre, Dalian, 116023, China
5   [2]School of Ocean Science and Technology, Dalian University of Technology, Panjin, 124221, China

Correspondence to: Ning Xu (11229585@qq.com)

Abstract. Sea ice disasters seriously threaten the safety of oil platforms in the Bohai Sea. Therefore, it is necessary to carry out the risk assessment of sea ice disasters on oil platforms in the Bohai Sea. In the study, a risk assessment of sea ice disasters on fixed jacket platforms in the Liaodong Bay was performed. Firstly, the formation mechanisms of sea ice disasters were

10   analyzed and the sources and modes of sea ice risks were clarified. Secondly, according to the calculation formulas of extreme ice force, dynamic ice force and accumulated force, several ice indices such as thickness, motion, strength, period, and concentration were proposed as the hazard indices and corresponding values were assigned to the proposed indices based on ice conditions in the Bohai Sea. Thirdly, based on four structural failure modes (structures overturned by the extreme ice force (Mode 1), structural fracture failure caused by dynamic ice force (Mode 2), the damage of facilities caused by the dynamic ice

15   force (Mode 3), and structural function failure caused by accumulated ice (Mode 4)), the structural vulnerability index, overturning index, dynamic index, ice-induced vibration index, and function index were proposed and corresponding values were assigned to the structural vulnerability index of fixed jacket platforms in the Liaodong Bay. Fourthly, the weight of each risk index was determined according to previous sea ice disasters and accidents and the sea ice risk was calculated with the weighted synthetic index method. Finally, with the above index system and risk assessment methods, the risk assessment of

20   sea ice disasters on 10 jacket platforms in three sea areas in the Liaodong Bay was carried out. The analysis results showed that efficient sea ice prevention strategies could largely mitigate the sea ice-induced vibration-related risks of jacket platforms in the Liaodong Bay. If steady-state vibration occurs (usually in front of the vertical legged structure) or the structural fundamental frequency is high, the structural vulnerability is significantly increased and the calculated risk levels are high. The sea ice risk assessment method can be applied in the design, operation, and management of other engineering structures

25   in sea ice areas.

1 Introduction

In recent years, the losses caused by sea ice disasters have increased significantly (Fang et al., 2017). In China, sea ice disasters mainly occur in the Bohai Sea and the North Yellow Sea. Sea ice can push down offshore platforms, destroy ships and offshore

30   engineering facilities, impede navigation, and cause losses to offshore and tidal aquaculture (Zhang et al., 2013; Wang et al.,

2011; Lu, 1993; Ding, 2000). In the ice period of 1969, the entire Bohai Sea was covered by sea ice and ice thickness even reached 60 cm. In the sea ice disaster, the No. 2 living and drilling platforms collapsed due to the huge thrust of sea ice, thus leading to a great impact on the economy of China. In 1977, the beacon tower of No. 4 drilling well was also pushed down by sea ice. On January 28, 2000, the JZ20-2 MS Platform suffered severe steady-state vibration under the action of level ice, thus

5   causing the fatigue fracture of the evacuation pipeline of the No. 8 well, natural gas leakage, and platform suspension (Yue et al., 2009; Li et al., 2008; Timco et al., 2011). Since 2010, the aquaculture area affected by sea ice disasters has reached 40,000 hectares per year (State Oceanic Administration, 2011-2016).

Since the 1980s, Chinese scholars studied the preventive measures of sea ice disasters (Ouyang et al., 2017; Lu et al., 1993; Wang et al., 2011; Zhang et al. 2015), sea ice measurement and forecast (Luo et al., 2004; Zhao et al., 2014; Su and Wang,

10   2012), engineering coping strategies (Zhang et al., 2010, 2016), and mechanisms (Yue et al., 2009; Li et al., 2008, Liu et al., 2009; Huang and Li, 2001; Wang et al., 2018; Yue et al., 2007a). Most studies on existing sea ice risk assessment only involved the descriptions of sea ice. Guo et al. (2008) proposed three sea ice parameters including thickness, strength and period as the influencing factors of sea ice disasters and established three sea ice disaster risk levels, such as zero risk, low risk, and high risk. Gu et al. (2013) converted sea ice thickness into a sea ice hazard index and determined sea ice hazard risk grades. However,

15   due to the differences in the classification results of sea ice disasters on different offshore engineering structures and dominant sea ice factors, the sea ice data required in the assessment of structural ice disaster are different. Therefore, previous results cannot meet the engineering requirements.

Risk assessment studies of engineering structures under environmental loads are mainly focused on large-span bridges, houses and other buildings under wind and seismic loads(Park et al., 1985; Schiff et al, 1994; Kameshwar et al, 2014.), and

20   corresponding vulnerability curves were obtained (Hwang and Liu, 2004; Singhal and Kiremidjian, 1996; Khanduri and Morrow, 2003). While there are little conclusions and applications of risk assessment studies of sea ice loads on marine platforms, no risk assessment indexes and method. The fundamental studies are mainly focused on ice force calculation methods (Sanderson, 1988; Ou et al, 2002), structural failure mode analysis (Yue et al, 2008), ice force resistance of engineering structures (Wang et al, 2012), and fatigue life calculation (Li et al, 2008; Liu et al 2006). The above work would

25   be the basic theory cfor the sea ice risk assessment indicator system and assessment method of marine structures.

This paper focuses on the risk assessment methods of sea ice disasters on jacket platforms. The hazard indices of sea ice were firstly determined according to the forms of sea ice force on platform structures. Then, the weight coefficients of these indices were determined with ice force calculation formulas. Then, the physical vulnerability index was determined according to the platform failure modes and the weight of the vulnerability index was determined based on the previous sea ice disasters and

30   accidents. Sea ice disaster risks on 10 jacket platforms in three sea areas were individually assessed with the overall risk assessment method and the multi-mode risk assessment method. Except that several auxiliary platforms are in the high risk level, other platforms are in the healthy condition, but safety management in winter should be further enhanced.

2 Study area

The Bohai Sea is a seasonal ice-covered sea in the latitude range of 37° and 41° N. It is also the ice-covered sea with the lowest latitude in the northern hemisphere. Liaodong Bay in the Bohai Sea is the most severely icy bay with the ice period of about 130 days. The edge of the ice-covered region is near the contour line of 15 m and about 70 nautical miles away from the top of the bay. Generally, ice thickness is 30-40 cm. The sea ice drifting speed is generally 0.5 m/s and the maximum speed is about 1.5 m/s. The dominant wind in winter is northerly wind. Due to clockwise flow along the coast and the right-turning tide, sea ice conditions in the east are heavier than those in the west. In addition, the warm current from Yellow Sea flows through the northern Bohai Strait into the Bohai Sea, and then to the west bank of Liaodong Bay roughly along the northwest direction, thus raising the water temperature in the western part of the Liaodong Bay. Therefore, sea ice conditions in the west of the Liaodong Bay are heavier than those in the east.

According to the distribution characteristics of sea ice in China, the Bohai Sea and the North Yellow Sea were divided into 21 regions in such a way that the ice conditions in each region were basically the same. Then, the design parameters of marine structures in the 21 regions areas were proposed, including physical and mechanical parameters as well as key parameters of ice conditions (period, thickness and motion). The sea ice parameters in each ice region provide a useful reference for the design of ice structures and the fatigue life assessment of existing structures.
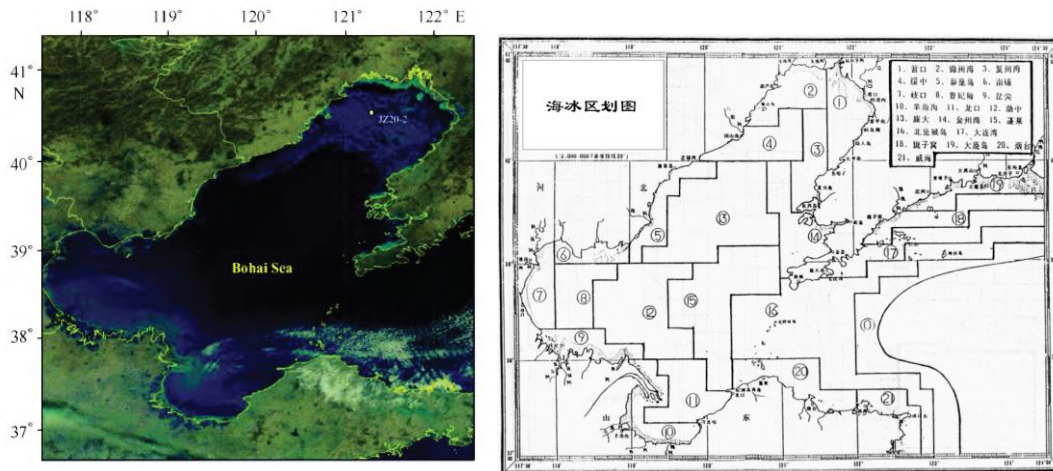
Fig. 1. Location map of Bohai Sea and North Yellow Sea.

Oil platforms in Bohai Sea have two structural categories: caisson structure and jacket structure. The latter is the dominant structure. In addition to the multi-legged structures (usually 4 legs, as shown in Fig. 2(a)), the single-legged structure has been widely applied in auxiliary platforms (Fig. 2(b)) and even main platforms (Fig. 2(c)). In oil platforms, ice-breaking cones are generally adopted to reduce the impact of sea ice. Old platforms had been equipped with ice-breaking cones (Fig. 2(d)) and new platforms were designed as the cone category (Fig. 2(e)). Due to the difference in ice conditions, structural category,

dynamic performance, function and structural ice resistance, platform structures in the Liaodong Bay showed significant differences in sea ice risk levels. Current sea ice management measures in winter effectively reduced sea ice risks in oil and gas exploitation.
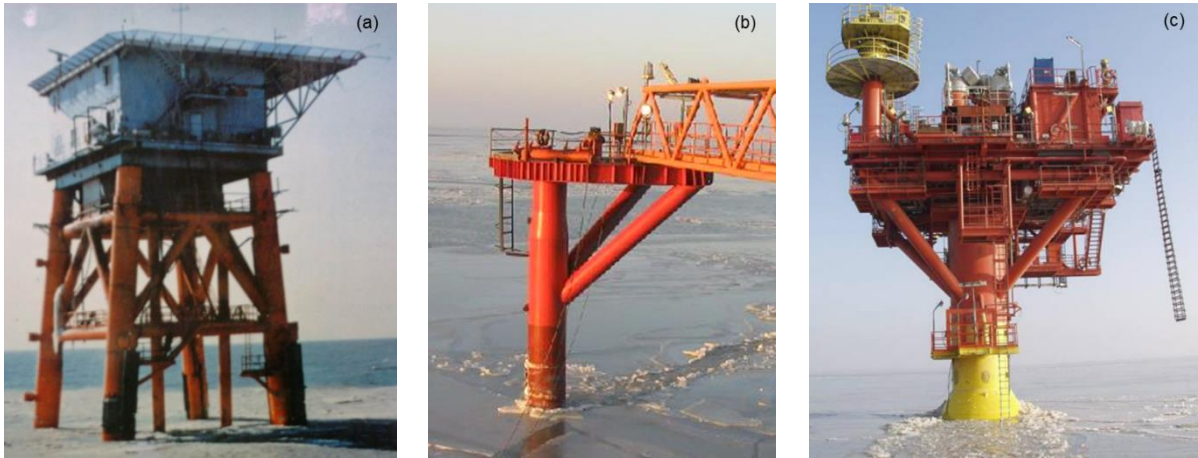
(a) Four-legged oil production platform (built in 1987); (b) One-legged auxiliary platform (built in 1999); (c) One-legged oil production platform (built in 2003).

(d) Three-legged upright pile production platform (built in 1997); (e) Three-legged upright pile production platform with cones (built in 2000)

Fig. 2. Main structural forms of jacket platforms in the Bohai Liaodong Bay.

Oil platforms are dense in the Liaodong Bay, especially the narrow form of jacket structures. The impact of sea ice is significant in the Liaodong Bay. Therefore, it is necessary to carry out the risk assessment of sea ice disasters on jacket oil platforms in the Liaodong Bay.

3 Research methods

3.1 Technical routes

According to the assessment method of natural disaster risks (Zhang et al., 2007; Tachiiri, 2012), the technical routine of the risk assessment of sea ice disasters on oil platforms was established below (Fig. 3).
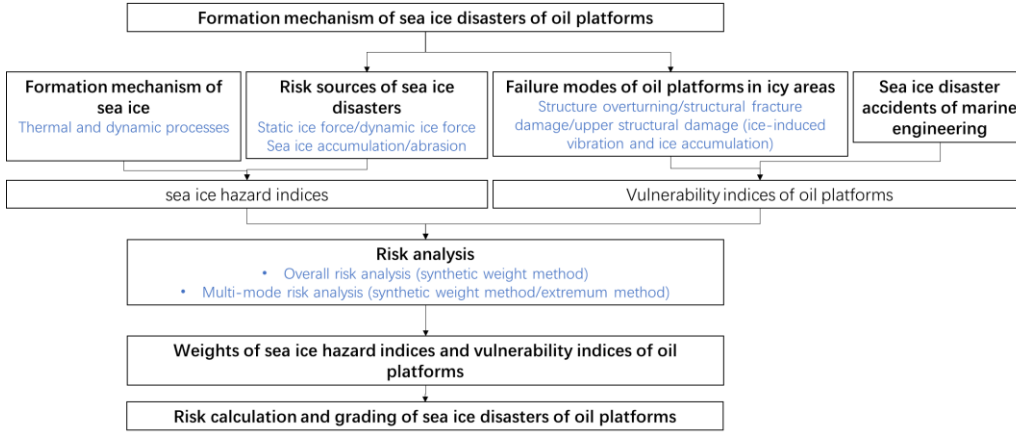
Fig. 3. Flow chart of risk assessment of sea ice disasters on oil platforms.

3.2 Risk assessment model index system

According to the synthetic index method (Zhang and Li, 2007), the sea ice risk assessment index system of oil platforms with the risk model was established (Risk = F (Hazard, Vulnerability, Resistance)) to calculate the risk. Firstly, the hazard index

10 (H), vulnerability index (V), and resistance index (R) were graded and corresponding values were assigned to these indices. Then the sea ice hazard index was qualitatively described as 5 levels: extremely high, high, medium, low, and extremely low and the corresponding quantitative values were respectively set to be 5, 4, 3, 2, and 1. The structural vulnerability index and the resistance levels were described qualitatively as 3 levels: high, medium and low and the corresponding values were set to be 5, 3, and 1, respectively.

15 Sea ice disasters on oil platforms have different risk modes. Therefore, in the establishment of risk assessment index systems and evaluation models, two methods can be adopted: overall risk assessment and multi-mode risk assessment. According to the overall risk assessment method, the weights of secondary indices are determined to calculate the hazard index (H), vulnerability index (V), and resistance (R) and then the overall risk I_e is calculated according to Eq. (1). According to the multi-mode risk assessment method, the assessment results of various risk modes $I_{s,i}$ are determined with the hazard index

20 H_i, the vulnerability index V_i, and the disaster resistance ability index R_i of various risk modes (Eq. (2)). Then, the risk result with the highest risk level $I_{s,max}$ can be calculated according to Eq. (3)). Finally, with the cumulative weight coefficient of various risk modes, the overall risk I_e or the highest risk level of various modes $I_{s,max}$ can be selected.

$$I_e = HVR = \sum \omega_i H_i \sum \omega_j V_j \sum \omega_k R_k \quad , \tag{1}$$

where I_e is the overall risk assessment result; H, V, and R are respectively the overall hazard, vulnerability, and disaster resistance ability indices; i, j, and k are respectively the numbers of H, V, and R secondary indices; H_i, V_j, and R_k are the secondary indices; ω_i, ω_j, and ω_k are respectively the weight coefficients of these secondary indices.

$$I_s = \sum \lambda_i I_{s,i} \quad , \tag{2}$$

$$I_{s,max} = max I_{s,i} \quad , \tag{3}$$

where I_s is the calculation result of the multi-mode risk assessment method; $I_{s,max}$ is the calculation result with the maximum risk value according to the multi-mode risk assessment; $I_{s,i} = H_i V_i R_i$ is the calculation result of the i-th risk mode; λ_i is the weight of the i-th risk mode.

4 Establishment of the risk assessment index system of sea ice disasters

4.1 Formation mechanisms of sea ice disasters

The impact of sea ice is the main cause for accidents and risks of marine structures in ice-covered areas. The impact energy mainly comes from wind, currents, thermal expansion and sea ice (Sanderson, 1988). Sea ice disasters have three major risk sources (extreme ice force, dynamic ice force, and sea ice accumulation) and four structural risk modes (structures overturned by extreme ice force, structural fatigue damage induced by ice vibration, upper facility damage by ice vibration, and facility damage due to ice pile climbing).

4.1.1 Risk sources of sea ice disasters and major sea ice risk factors

4.1.1.1 Extreme ice force

When sea ice contacts a structure and maintains its integrity, sea ice exerts a relatively stable ice force on the structure. Extreme ice force generates static effects and transient impacts. In the sea areas around oil platforms in the Liaodong Bay, sea ice flow rate can reach 1.4 m/s and extreme ice force is directly affected by sea ice thickness, sea ice strength and structural width. The calculation methods of static ice force are given in various engineering design standards of cold zones. For example, when ice is crushed in front of a structure, the ice load generated on the structure can be calculated (API, 1995) as follows:

$$F_c = mI f_c \sigma_c DH, \tag{4}$$

where F_c is extrusion ice load; m is shape factor and respectively set as 0.9, 1.0 and 0.7 for circular section, square section with positively applied ice load and square section with obliquely applied ice load; I is the embedding coefficient; f_c is the

contact coefficient; σ_c is the uniaxial compression strength of level ice in the horizontal direction, MPa; D is structural width; H is the designed level ice thickness.

The horizontal component of ice bending load applied on a slope structure is:

$$F_H = K_\alpha H^2 \sigma_f tan\beta, \tag{5}$$

where F_H is the horizontal component of ice bending load applied on a slope structure; K_α is the coefficient related to the structure and ice thickness; H is the designed level ice thickness; σ_f is bending strength of level ice; β is the angle (°) between the structural slope and the horizontal plane (RIL, 2001).

4.1.1.2 Dynamic ice force

When sea ice continuously passes through a structure, it generates a periodic impact load on the structure, namely, dynamic ice force. Dynamic ice force usually occurs on narrow structures. Under the action of dynamic ice force, a structure will undergo vibration, namely, ice-induced vibration. When the frequency of dynamic ice force is consistent with the structural frequency, it will cause strong vibration due to resonance. Based on the measured ice force time history, the ice force calculation method is proposed (Qu et al., 2006). Ice force amplitude and ice force period are important parameters in the calculation. Ice force amplitude can be calculated based on the calculation method of extreme ice force. The recommended calculation method of ice force period is provided in Eq. (6) (Qu et al., 2006).
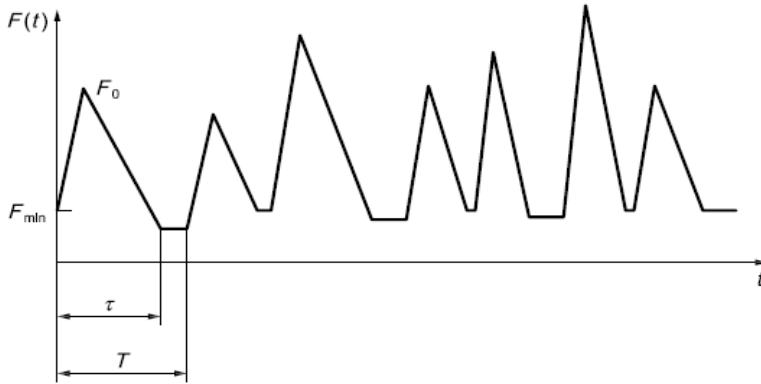
Fig. 4. Time history curve of dynamic ice force on a typical coned structure.

$$T = l_b/v, \tag{6}$$

where T is ice force period; l_b is breaking length of ice plate and affected by ice thickness, ice strength, structural diameter, and ice velocity; v is ice velocity.

4.1.1.3 Sea ice accumulation

After floe is applied on a structure and then broken, if broken ice is not removed in time due to structural blockage, ice accumulation will occur. Usually, the accumulation of broken ice occurs in front of a wide structure or in the vicinity of dense

ice-collecting members, such as spacing casing group of the pile leg of an oil platform and the coarse grid at the water intake port of a nuclear power plant. The growth, size, and load of accumulation ice had been extensively explored. The calculation methods of extreme ice force in various specifications also involve ice accumulation. Sea ice accumulation height is calculated as follows (Brown and Määttänen, 2009):

$$H = 3 + 4h \ , \tag{7}$$

$$H = 7.6h^{0.64}, \tag{8}$$

where h is level ice thickness.

4.1.2 Sea ice risk modes and key structural parameters of oil platforms

4.1.2.1 Extreme ice force may cause the overall structural failure

When the overall deformation of a structure exceeds its allowable deformation under extreme ice force, structural stiffness failure occurs. When extreme ice force exceeds the ultimate bearing capacity of a structure, the structure may be unstable.

4.1.2.2 Ice-induced vibration may cause structural fatigue failure

Structural fatigue damage is caused by a stress repeatedly applied at pipe joints, which are called hot spots. Structural hot spots fails after the significant stress (S) has been applied for the specified times (N). Long-term ice-induced structural fatigue damage may decrease the structural resistance and even cause the structural failure due to insufficient structural resistance. In general, conventional ice loads with a higher probability cause a greater damage to a platform structure, whereas extreme ice loads with a lower probability have a smaller effect on the platform.

4.1.2.3 Dynamic ice force may lead to the function failure of facility and affect personnel safety

The strong ice-induced vibration of a structure directly affects its upper facility. In such a vibration, the platform deck is equivalent to the vibration table and can cause the whiplash effect on the upper components. Especially, ice-induced vibration may lead to the direct damage to the key functional facility or components without anti-vibration capability. Natural gas pipelines are distributed on the upper part of platforms for producing natural gas. Due to the long-term ice-induced vibration, connecting parts of these pipelines may be weakened, thus causing natural gas leakage, pipeline breaking and even explosion. The impacts of ice-induced vibration on workers include slight impact, reduced comfort, reduced efficiency, and affected health.

4.1.2.4 Sea ice accumulation may cause the damage to the upper facility or buildings

Sea ice accumulation will increase the application area of ice force on marine structures as well as ice force itself. If sea ice climbs to a structure at a certain height from the ice surface along accumulated ice, it may cause the damage to the upper facility or buildings. If sea ice climbs to a dam, it will destroy onshore buildings. If sea ice climbs to the underlying cable aisle of a platform, sea ice may crush the fence and affect the overall structural stability.

4.2 Hazard index system

4.2.1 Determination of hazard indices based on the risk analysis of sea ice disasters

Based on the relationships among sea ice parameters and their contributions to ice force, the key sea ice hazard indices were proposed (Table 1). Short-term sea ice hazard indices that play a key role in the failure of the platform structure include thickness, velocity, and strength. The long-term sea ice hazard indices related to the time and frequency of sea ice load include ice period and sea ice concentration.

Table 1. Sea ice hazard indices.

Index types	Indices	Criteria
Short-term sea ice hazard indices	Ice thickness, ice velocity, and ice strength	Indices that play a key role in the failure of the platform structure
Long-term sea ice hazard indices	Ice period and sea ice concentration	Indices related to the time and frequency of sea ice load

4.2.2 Sea ice hazard indices

According to Technical Guidelines for Risk Assessment and Zoning of Sea Ice Disasters (State Oceanic Administration, 2016), sea ice hazard indices were graded. The study area was divided into 21 regions and the values of the indices in each region were mainly determined based on the China Sea Ice Conditions and Application Regulations (Q/HSn 3000-2002). Since the designed life of the oil platform in Bohai Sea was 100 years, a return period of 100 years was selected in the subsequent analysis.

Table 2. Grading of sea ice hazard indices.

Index code	Indices	Index range	Extremely high hazard (5 points)	High hazard (4 points)	Medium hazard (3 points)	Low hazard (2 points)	Extremely low hazard (1 point)
H_1	Designed ice thickness, cm	8~41.7	>35	[35,25)	[25,10)	[10,5)	≤5
H_2	Designed ice velocity, cm·s^{-1}	0.7~1.9	>1.4	[1.4,1.2)	[1.2,1.0)	[1.0,0.8)	≤0.8
H_3	Designed ice strength, Mpa	1.88~2.37	>2.2	[2.2,2.1)	[2.1,2.02)	[2.02,1.9)	≤1.9
H_4	Designed severe ice period, day	30~149	>35	[35,25)	[25,10)	[10,5)	≤5
H_5	Maximum ice concentration,%	0~100	>80	[80,60)	[60,40)	[40,20)	≤20

4.3 Vulnerability indices

4.3.1 Determination of vulnerability indices based on the failure mode of jacket structures

According to typical sea ice disaster risk modes, the assessment index by various structural failure modes (M_1, M_2, M_3, M_4), Structural vulnerability index (V_1, V_2, V_3, V_4) affecting sea ice disasters are proposed for the first time, and the above assessment indexes are calculated by the structural parameters (Table 3) and the structural influencing factors are analyzed. The main failure modes of jacket structures includes structure overturning by extreme ice force, structural fatigue damage caused by dynamic ice force, and the damage to the upper facility (including personnel) caused by dynamic ice force. Yue et al. (2007b) analyzed the static displacement of typical platforms in the Liaodong Bay under extreme ice force.

Table 3. Sea ice disaster risk modes of oil platforms and corresponding vulnerability indices.

Risk modes	Structural performances	Assessment index by various structural failure modes	Structural vulnerability index	Structural parameters	Section
Structure overturning by the extreme ice force	Anti-overturning ability	Overturning index $M_1=V_1$	Overturning index $V_1=K_n/KH$	H,overall height of the structure; K, structural stiffness; K_n, coefficient	4.3.1.1
Structural fatigue damage caused by the dynamic ice force	Ice-induced vibration resistance capacity (displacement and strain)	the structural dynamic value corresponding to structural ice vibration fatigue $M_2=V_1*V_2$	Overturning index $V_1=K_n/KH$ Dynamic index $V_2=\gamma_1*K_a$	Above γ_1, dynamic amplification factor; K_a, coefficient of hot spots, (0,1]	4.3.1.2
The facility damage caused by the dynamic ice force	Ice-induced vibration resistance capacity (acceleration)	The ice-induced vibration value M_3 $M_3=V_1*V_2*V_3*V_40.5$	Overturning index $V_1=K_n/KH$ Dynamic index $V_2=\gamma_1*K_a$ Ice-induced vibration index $V_3=f_2$, Function index $V_4=K_b$	Above f, first natural frequency for jacket structures K_b, the structural function coefficient, 1.5, 1.2, and 1.0	4.3.1.3
Structural function failure caused	Structural function	Damage to the upper facility of the structure	Function index $V_4=K_b$	K_b, the structural function coefficient, 1.5, 1.2, and 1.0	4.3.1.4

by	caused by sea ice
accumulation	accumulation $M_4=V_4$
ice	

4.3.1.1 Structural overturning by extreme ice force (Mode 1) and structural overturning index

When extreme ice force exceeds the ultimate bearing capacity of a structure, the whole structure collapses. The overturning index V_1 is proposed below.

Based on functional descriptions of buildings under seismic loads, the damage of a structure under extreme ice load is provided in Table 4.

Table 4. Damages of marine structures under extreme ice loads.

Functional levels	I	II	III	IV	V
Damage states	Basically intact	Slight damage	Medium damage	Severe damage	Collapse
Relative structural deformation	$\Delta < H/500$	$H/500 < \Delta < H/250$	$H/250 < \Delta < H/125$	$H/125 < \Delta < H/50$	$\Delta > H/50$

Note: $\Delta=F/K$, where F is ice force; K is structural stiffness; H is the overall height of the structure.

When the ice force difference is not large (10~100 kN), the overturning index of the platform under extreme ice force is proposed as:

$$M_1=V_1=K_n/KH, \tag{9}$$

where H is the overall height of the structure; K is structural stiffness and it is set to be 10e7~10e9 for jacket platforms in the Liaodong Bay; K_n is the coefficient related to the structural form (pile) and its values for the one-legged platforms and 4-legged platforms are respectively set to be 1 and 2.

4.3.1.2 Structural fatigue damage caused by dynamic ice force (Mode 2) and structural dynamic index

Structural fatigue damage is caused by a stress repeatedly applied at hot spots of pipe nodes. For jacket structures, the stress applied at hot spots is usually linear with structural dynamic response (Δd), which is proportional to the static loading deformation ($\Delta=F/K$). The proportional coefficient is called the amplification factor γ and directly related to structural natural frequency and ice force frequency. Yue et al. (2007b) analyzed the dynamic characteristics of anti-ice jacket platforms in the Bohai Sea. For the steady-state vibration of an upright structure, the amplification factor is:

$$\gamma = \frac{1}{\sqrt{(1-r^2)^2+(2\xi r)^2}}. \tag{10}$$

For the random vibration of coned structures, the amplification factor is:

$$\gamma_1 = \frac{1}{5\sqrt{(1-r_1^2)^2 + (2\xi r_1)^2}}, \tag{11}$$

where both r and r_1 are the frequency ratio, $r_1=\omega/\omega_n=f/f_n$; $\omega(f)$ and $\omega_n(f_n)$ are respectively ice force frequency and structural natural frequency.

The structural dynamic index V_2 is calculated as:

$$V_2=\gamma_1*K_a, \tag{12}$$

where γ_1 is dynamic amplification factor and can be calculated with the measured data or frequency ratio ($\gamma_1=f(\gamma_1,\xi)$) according to Eqs. (10) and (11); K_a is the reinforcement coefficient of hot spots, namely, the ratio of the stress at the hot spot before reinforcement to that after reinforcement, and its range is (0,1]. Based on finite element analysis or measured data, in the study, the values of Ka were respectively selected as 0.5 for main platforms and satellite platforms and 1.0 for auxiliary platforms.

Considering the fatigue failure modes of jacket structures under dynamic ice force, with structural overturning index V_1 and dynamic index V_2, the structural dynamic value corresponding to structural ice vibration fatigue is expressed as:

$$M_2=V_1*V_2, \tag{13}$$

where $V1$ is calculated according to Eq. (9).

4.3.1.3 Damage to the upper facility (including personnel) caused by dynamic ice force (Mode 3)

In general, the greater deck acceleration leads to the greater vibration amplitude of the facility. If it is believed that a jacket structure can be simplified as a structure with a single degree of freedom (Yue, 2007b), deck vibration is similar to simple harmonic motion and its vibration displacement D, velocity V, and acceleration A can be respectively expressed as:

$$D = \Delta st \times sin(\omega t + \varphi); \tag{14}$$

$$V = \Delta st \times \omega \times cos(\omega t + \varphi); \tag{15}$$

$$A = -\Delta st \times \omega^2 \times sin(\omega t + \varphi). \tag{16}$$

In Mode 2, vibration displacement D corresponding to structural vibration index is the key factor to be considered. In the analysis of Mode 3, structural dynamic parameter, natural frequency f, should be carefully considered. The higher structural frequency means the greater acceleration. In addition, the structural function also directly affects the risk level. For example, there are many devices on oil production platforms. The design of manned platforms should pay attention to personnel comfort and their risk is relatively high. Unmanned platforms have a low risk. In summary, structural ice vibration index V_3 and structural function index V_4 are proposed respectively based on natural frequency and structural function as follows:

$$V_3=f^2, \tag{17}$$

where f is the dominant ice vibration frequency of a platform, which is the first natural frequency for jacket structures.

$$V_4 = K_b, \tag{18}$$

where K_b is the structural function coefficient and its values for manned central platforms, unmanned central platforms, and auxiliary function platforms such as the bollard are respectively set to be 1.5, 1.2, and 1.0.

5   In Mode 3, the vibration and functions of a structure should be considered. The structural vulnerability indices to be considered include overturning index V_1, dynamic index V_2, ice-induced vibration index V_3, and function index V_4. The ice-induced vibration value M3 is expressed as:

$$M_3 = V_1 * V_2 * V_3 * V_4^{0.5}, \tag{19}$$

where V_1, V_2, V_3, and V_4 are respectively calculated according to Eqs. (9), (12), (17), and (18).

10   Because the contribution of V_4 (Function index) is lower than other 3 Structural vulnerability indexes (V_1 Overturning index, V_2 Dynamic index, V_3 Ice-induced vibration index), so the author added the 0.5 times power on V_4.

4.3.1.4 Damage to the upper facility of the structure caused by sea ice accumulation (Mode 4)

If sea ice climbs to the platform deck due to sea ice accumulation, it will directly threaten the safety of facilities and personnel. Therefore, the vulnerability index mainly considered in Mode 4 is the functional index V_4.

15    $$M_4 = V_4 \ . \tag{20}$$

4.3.2. Vulnerability indices

According to the main distribution ranges of the parameters of jacket platforms in the Liaodong Bay, the above-mentioned structural vulnerability indices proposed based on the sea ice risk modes of oil platforms are graded into three levels: high, medium and low (Table 5).

20   **Table 5. Grading and assignment of structural vulnerability indices.**

Index codes	Indices	Index range	High risk (5 points)	Medium risk (3 points)	Low risk (1 point)
V_1	Overturning index	[4e-10,7e-9]	>2e-9	[2e-9, 1e-9)	⩽ 1e-9
V_2	Dynamic index	[2,12]	>4	[4,2)	⩽ 2
V_3	Ice-induced vibration index	[0.5,5]	>4	[4,1.0)	⩽ 1.0
V_4	Function index	[1,1.5]	1.5	1.2	1

4.4 Disaster resistance ability index

Emergency monitoring and sea ice management measures are the important factors to be considered in the assessment. The disaster resistance ability index R_1 is proposed (Zhang et al, 2012) and graded in three levels (Table 6).

Table 6. Grading and assignment of disaster resistance ability index.

Index code	Index	Invalid I	Partially valid II	Valid III
R_1	Disaster resistance ability index	1.0	(0.5, 1.0)	0.5

4.5 Risk assessment method

Before the risk assessment of sea ice disasters, it is necessary to separately determine the index system, assessment models, and grading standards. The index system varies with the evaluation model. The index systems are introduced separately according to the overall risk assessment method and the multi-mode risk assessment method below.

4.5.1 Overall risk assessment method

The weight coefficients of sea ice hazard indices were determined according to the importance of each index in the ice force calculation models (Table 7). The weights of structural vulnerability indices (Table 7) were determined based on the failure modes of structures and the probabilities of corresponding risks or accidents (Table 8).

Table 7. Hierarchical structure and weights of sea ice risk assessment factors for overall risk analysis.

Criteria layer	Index codes	Sub-criteria layer	Index codes	Weights	
Sea ice hazard indices	H	Designed ice thickness	W_1	0.69	
		Designed ice velocity	W_2	0.02	
		Designed ice strength	W_3	0.06	1
		Maximum ice concentration	W_4	0.1	
		Designed severe ice period	W_5	0.13	
Structural vulnerability indices	V	Overturning index	Q_1	0.45	
		Overturning index	Q_2	0.39	
		Ice-induced vibration index	Q_3	0.09	1
		Functional index	Q_4	0.07	
Structural resistance	R	Structural resistance index		0.1	

Table 8. Probability of platform failure modes and weight coefficient assignment.

Platform failure modes	Probability	Assessment index assignment	Weight coefficients			
			V_1	V_2	V_3	V_4
Structures overturned by extreme ice force	6%	Overturning index assignment, $M_1=V_1$.	0.06	/	/	/

Dynamic ice force causes structural fatigue damage	60%	Dynamic index assignment, $M_2=V_1*V_2$.	0.3	0.3	/	/
Dynamic ice force causes the damage to the upper facility (personnel) of structures	30%	Ice-induced vibration index assignment, $M_3=V_1*V_2*V_3*V_4^{0.5}$.	0.09	0.09	0.09	0.03
Accumulated ice causes the damage to the upper facility of structures	4%	Function index assignment, $M_4=V_4$.	/	/	/	0.04
Total	100%		0.45	0.39	0.09	0.07

4.5.2 Multi-mode risk assessment method (multi-index synthetic risk assessment model)

Firstly, the weights of various risk modes were determined based on the failure modes of sea ice disasters and the probabilities of corresponding risks or accidents. Then, based on risk sources, risk mode assignments, and disaster resistance ability in various failure modes, the weights of the hazard indices, vulnerability indices, and disaster resistance ability indices were respectively determined (Table 9).

Table 9. Hierarchical structure and weights of sea ice risk assessment factors for multi-mode risk analysis.

Criteria layer	Index codes	Sub-criteria layer	Index codes	Weight coefficients	Key index layer	Index codes	Weight coefficients
Structures overturned by extreme ice force (0.06)	R_1	Extreme ice force	H_1	0.20	Ice thickness	$H_{1.1}$	0.20
		Anti-overturning capability of a platform	V_1	0.30	Structural overturning index	$V_{1.1}$	0.30
		Disaster resistance ability	R_1	1.00	Disaster resistance ability index	$R_{1.1}$	1.00
Damage to the main structure caused by ice-induced vibration (0.60)	R_2	Dynamic ice force and its influencing scope (temporal and spatial distributions)	H_2	1.00	Ice thickness	$H_{2.1}$	0.8
					Ice period	$H_{2.2}$	0.2
		Anti-overturning capability of a platform	V_2	0.60	Structural overturning index	$V_{2.1}$	0.30
					Dynamic index	$V_{2.2}$	0.30
		Disaster resistance ability	R_1	1.00	Disaster resistance ability index	$R_{2.1}$	1.00
Damage to the upper facility caused by ice-	R_3	Dynamic ice force and its influencing scope	H_3	0.50	Ice thickness	$H_{3.1}$	0.30
					Ice concentration	$H_{3.2}$	0.10
					Ice period	$H_{3.3}$	0.10

induced vibration (0.30)		Anti-overturning capability and function of a platform	V_3	0.60	Structural overturning index	$V_{3.1}$	0.18
					Structural dynamic index	$V_{3.2}$	0.18
					Ice-induced vibration index	$V_{3.3}$	0.18
					Function index	$V_{3.4}$	0.06
		Disaster resistance ability	R_1	1.00	Disaster resistance ability index	$R_{3.1}$	1.00
Damage to the facility caused by accumulation ice (0.04)	R_4	Ice accumulation	H_4	0.50	Ice thickness	$H_{4.1}$	0.40
					Ice concentration	$H_{4.2}$	0.1
		Function of a platform	V_4	0.08	Function	$V_{4.1}$	0.08
		Disaster resistance ability	R_1	1.00	Disaster resistance ability index	$R_{4.1}$	1.00

4.6 Assessment calculation method and grading criteria

According to Eqs. (1) to (3) in Section 3.2, the risk was calculated with the overall risk analysis method and then graded into 4 levels. The criteria and results of the risk assessment of sea ice disasters on oil platforms are proposed in this study (Table 10).

Table 10. Assessment criteria of the risks of sea ice disasters on the oil platforms in the Bohai Sea.

Risk index	(12, 25]	(9, 12]	(6, 9]	[0.5, 6]
Levels	Severe risk	Moderate risk	Mild risk	Low risk

5 Case analysis

5.1 Parameters

Taking 10 jacket platforms with different functions in the three regions of Liaodong Bay (JZ20-2, JZ21-1, and JZ9-3) as the cases, sea ice risks were calculated with the above assessment methods. The vulnerability index was determined according to the locations of the three regions and corresponding sea ice parameters (Table 11). The designed and assigned values of the vulnerability indices of the 10 platforms were determined by the basic forms, functions and dynamic parameters of the platforms (Table 12).

Table 11. Designed and assigned values of sea ice hazard indices in case analysis

Indices	Sea regions	Sea Region 20-2	Sea Region 21-1	Sea Region 9-3
Designed ice thickness (H_1)	Designed values/cm	41.7	40.4	36.8
	Assigned values	5	5	5

Designed ice velocity (H_2)	Designed values /cm · s^{-1}	1.9	1.8	1.4
	Assigned values	5	5	4
Designed ice strength (H_3)	Designed values /Mpa	2.37	2.16	2.33
	Assigned values	5	5	5
Designed severe ice period (H_4)	Designed values /day	85	53	72
	Assigned values	5	5	5
Maximum ice concentration (H_5)	Designed values /%	almost 100	almost 100	80
	Assigned hazard values	5	5	5

Platforms		JZ20-2 A	JZ20-2 B	JZ20-2 C	JZ20-2 D	JZ21-1 E	JZ9-3 F	JZ9-3 G	JZ9-3 H	JZ9-3 I	JZ9-3 J
No. of legs		4	3	4	1	4	4	1	4	1	1
Leg forms	(Cone or Cylinder)	cone	cone	cone	cone	cone	cone	cylinder	cone	cylinder	cone
Platform functions	(Oil recovery/auxiliary function)	Oil recovery	Oil recovery	Oil recovery	Oil recovery	Oil recovery	Auxiliary compressor	Auxiliary mooring pile	Oil recovery	Auxiliary mooring pile	Oil recovery
Manned/unmanned		Manned	unmanned	Manned	Manned	unmanned	unmanned	unmanned	Manned	unmanned	unmanned
Leg coefficients	k_n	1.5	2	1.5	1	1.5	1.5	1	1.5	1	1.2
Static stiffness	K	2.00E+08	6.40E+07	9.30E+07	6.10E+07	9.00E+07	1.20E+08	1.30E+08	9.00E+07	5.40E+07	2.10E+07
Water depth	H	15.6	16.5	16.5	13.5	15.6	9.5	10	9	9	9
Amplification coefficient	γ	4.17	4.17	4.17	4.17	4.17	6	12	4.17	4.17	15
Ice-breaking coefficient	K_a	0.5	0.5	0.5	0.5	0.5	1	1	0.5	1	0.5
Natural frequency	f	0.87	1.36	1.41	1	1.1	2.06	2.32	1.1	6.4	0.84
Function coefficient	K_b	1.5	1.2	1.5	1.5	1	1.2	1	1.5	1	1.2

Anti-overturning index	$V_1=k_n/(KH)$	4.80E-10	1.90E-09	9.80E-10	1.20E-09	1.10E-09	1.30E-09	7.60E-10	1.90E-09	2.10E-09	6.50E-09
	Assigned values	1	3	1	3	3	3	1	3	5	5
Dynamic index	$V_2=K_a*\gamma$	2.08	2.08	2.08	2.08	2.08	6	12	2.08	4.17	7.5
	Assigned values	3	3	3	3	3	5	5	3	5	5
Ice-induced vibration index	$V_3=f^2$	0.76	1.85	1.99	1	1.21	4.24	5.38	1.21	40.96	0.71
	Assigned values	1	3	3	1	1	5	5	3	5	1
Function index	$V_4=k_b$	1.5	1.2	1.5	1.5	1	1.2	1	1.5	1	1.2
	Assigned values	5	3	5	5	1	3	1	5	1	3

5.2 Sea ice risk assessment and grading

According to the overall risk analysis method described in Section 4.4.1, the sea ice hazard (H), structural vulnerability (V) and disaster resistance ability (R) were determined and then the overall risk I_e was calculated according to Eq. (1) and Table 7. Then, the calculation results of four sea ice risks $I_{s,i}$ (i=1,2,3,4) were determined. According to Eqs. (2) and (3), with the synthetic index method, the multi-mode risk analysis results I_s and maximum risk values $I_{s,max}$ were calculated.

Table 13. Sea ice risk assessment analysis and risk grading results in case analysis.

Platforms	Overall risk analysis				Multi-mode risk analysis					
	H	V	R	$I_e=HVR$	$I_{s,1}$	$I_{s,2}$	$I_{s,3}$	$I_{s,4}$	$I_{s,max}$	$I_{s,c}$
JZ20-2 A	5	2.06	0.5	5.15	2.5	5	5	12.5	12.5	5.15
JZ20-2 B	5	3	0.5	7.5	7.5	7.5	7.5	7.5	7.5	7.5
JZ20-2 C	5	2.24	0.5	5.6	2.5	5	6.5	12.5	12.5	5.6
JZ20-2 D	5	2.96	0.5	7.4	7.5	7.5	6.5	12.5	12.5	7.4
JZ21-1 E	5	2.68	0.5	6.7	7.5	7.5	5.5	2.5	7.5	6.7
JZ9-3 F	4.98	3.96	0.5	9.86	7.5	10	11	7.5	10.5	9.9
JZ9-3 G	4.98	2.92	0.5	7.27	2.5	7.5	8.5	2.5	8.5	7.3
JZ9-3 H	4.98	3.14	0.5	7.82	7.5	7.5	8	12.5	12.5	7.85
JZ9-3 I	4.98	4.72	0.5	11.8	12.5	12.5	12	2.5	12.5	11.8
JZ9-3 J	4.98	4.5	0.5	11.2	12.5	12.5	9	7.5	12.5	11.25

Notes: ■ indicates severe risk; ■ indicates moderate risk; ■ indicates mild risk; ■ indicates low risk.

5.3 Analysis results

The three risk calculation results (I_e, I_s, and $I_{s,max}$) were compared (Fig. 5). In the calculation results obtained by the synthetic index method, the overall risk analysis results I_e were basically the same to the multi-mode risk analysis results I_s and the risk grading results were the same because the theoretical basis for establishing the index system and the weight of the secondary indices were the same in the two methods. The risk mode with the higher weight (such as Mode 2) dominated the multi-mode risk analysis results (I_s) obtained with the synthetic index method. When $I_{s,max}$ was largely different from I_e and I_s, the risk values of most of the risk modes (such as Mode 4) with lower weights were higher, such as Platforms A, C, D, and H.
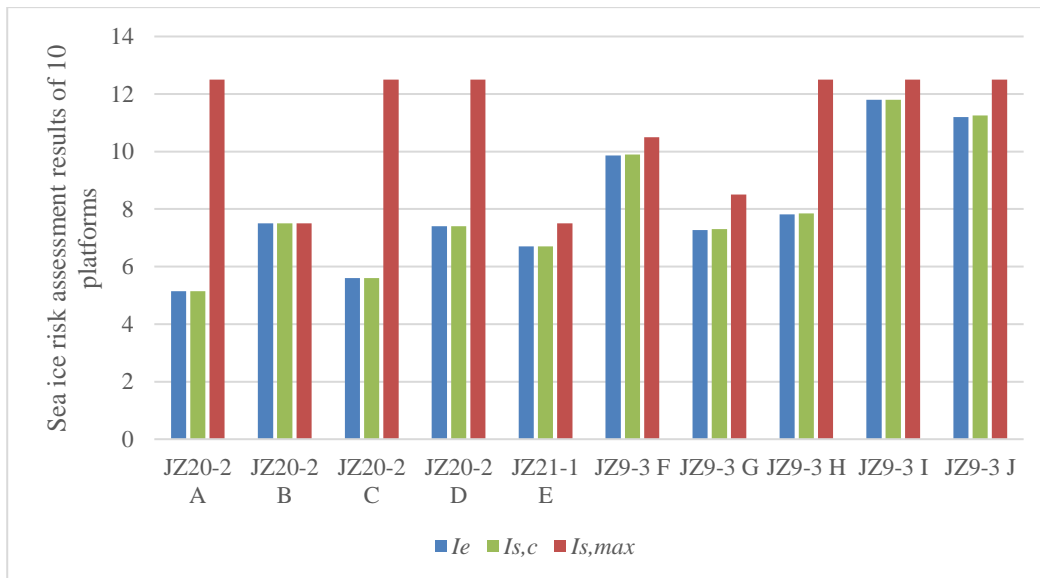
Fig. 5. Comparison of the three risk calculation results (I_e, I_s, and $I_{s,max}$).

According to the overall risk analysis results I_e and the multi-mode risk analysis results I_s, there are two main reasons for the higher risk level. Firstly, the steady-state vibration may occur on the structures and the dynamic larger amplification factor γ leads to the higher dynamic index V_2. Therefore, the structural fatigue failure related to ice-induced vibration caused by dynamic ice force (Mode 2) occurs on some platforms, such as Platforms F and J. Secondly, due to the high structural fundamental frequency, the structural ice-induced vibration index V_3 is large and the facility function failure caused by ice-induced vibration acceleration (Mode 3) occurs. For example, Platform I has a fundamental frequency of 6.4 Hz, which is significantly higher than the fundamental frequency of common jacket structures in the Liaodong Bay (0.5~2 Hz).

6 Conclusions

In the study, the risk assessment method of sea ice disasters was developed for jacket platforms in ice-covered sea areas in the Liaodong Bay of Bohai Sea. The sea ice risk index system considering sea ice hazard, structural vulnerability and disaster

resistance ability was established. In addition, based on the synthetic index method, sea ice disaster assessment methods were constructed, including the overall risk assessment method and multi-mode risk assessment method. The above key indices were determined based on the formation mechanism of sea ice disasters. The weights of these indices were recommended based on sea ice disaster cases. The conclusion could be on rafted ice, while the variance of ice property parameters value

5   should be paid attention

This paper focus on the structural risk induced by level ice, based on the formation mechanisms of sea ice disasters, which is the level ice failure process while interacting on structures and level ice force on structures. The method could also be used on rafted ice because of the similar ice-structure interaction process with level ice. While the variance of ice property parameters value should be paid attention. Meanwhile the values of these indices were determined based on the ice

10   conditions and parameters of jacket platforms in the Liaodong Bay. The applicability of these values in other sea areas needs to be further verified.

Acknowledgement

This study is financially supported by The National Key Research and Development Program of China (Grant No. 2017YFQ0604902), Public Science and Technology Research Funds Projects of Ocean (Grant No. 201505019), and National

15   Natural Science Foundation of China (Grant No. 41676087).

References

API, API RP 2N: Recommended practice for planning, designing, and constructing structures and pipelines for arctic conditions, American Petroleum Institute, 1995.

Brown T. G. and Määttänen, M.: Comparison of Kemi-I and Confederation Bridge cone ice load measurement results[J]. Cold

20   Regions Science & Technology, 2009, 55(1):1-13.

Ding, D.W.: Introduction to sea ice engineering, China Ocean Press, Beijing, 1–70, 2000.

Fang, J., Liu, W., Yang, S., Brown, S., Nicholls, R. J. and Hinkel, J.: Spatial-temporal changes of coastal and marine disasters risks and impacts in mainland china. Ocean and Coastal Management, 139(10), 125-140, 2017.

Gu, W., Liu, C., Yuan, S., Li, N., Chao, J. and Li, L.: Spatial distribution characteristics of sea-ice-hazard risk in Bohai, China.

25   Annals of Glaciology, 54(62), 73-79, 2013.

Guo, Q. Z., Gu, W. and Li, J.: Research on the sea–ice disaster risk in Bohai Sea based on the remote sensing, J Catastrophol, 23(2),10–18, 2008.

Huang, Y. and Li, X.: Dynamic ice loads on conical structures. Ocean Engineering, 1(2), 022007, 2011.

Hwang, H. and Liu, Ji.: Seismic fragility analysis of reinforced concrete bridges. China Civil Engineering Journal, 37(6), 47-

30   51, 2004.

Kameshwar, S. P. and Jamie, E.: Multi-hazard risk assessment of highway bridges subjected to earthquake and hurricane hazards. Engineering Structures, 78(1), 154-166, 2014.

Khanduri, A. C and Morrow, G. C.: Vulnerability of buildings to wind storms and insurance loss estimation. Journal of Wind Engineering and Industrial Aerodynamics, 91(4), 455-467, 2003.

Li, G., Liu, X., Liu, Y. and Yue, Q.: Optimum design of ice-resistant offshore jacket platforms in the Bohai Gulf in consideration of fatigue life of tubular joints. Ocean Engineering, 35(5), 484-493, 2008.

5   Li, G., Liu, X., Liu, Y., and Yue, Q.: Optimum design of ice-resistant offshore jacket platforms in the bohai gulf in consideration of fatigue life of tubular joints. Ocean Engineering, 35(5), 484-493, 2008.

Liu, X., Li, G., Yue, Q., and Oberlies, R.: Acceleration-oriented design optimization of ice-resistant jacket platforms in the bohai gulf. Ocean Engineering, 36(17), 1295-1302, 2009.

Liu, Y., Yue, Q. J., Yan, Q. U., Wang, R. X. and Yu, X. B.: Estimation of ice-reduced fatigue life for ice-resistant jacket

10   platforms. Ocean Engineering.

Lu, T. N., Sea ice disaster and its countermeasures of Bohai in China, Journal of Natural Disasters, 4, 53-59, 1993.

Luo, Y. W., Wu, H. D., Zhang, Y. F., Sun, C. R. and Liu, Y.: Application of the hy-1 satellite to sea ice monitoring and forecasting. Acta Oceanologica Sinica, 23(3), 251-266, 2014.

Ouyang, L. X., Hui, F. M., Zhu, L. X., Cheng, X., Cheng, B., Shokr, M., Zhao, J. Ding, M. H. and Zeng, T.: The spatiotemporal

15   patterns of sea ice in the Bohai Sea during the winter seasons of 2000–2016, International Journal of Digital Earth , 1-17, 2017.

Park, Y. J., Ang, A.H. and Wen, Y.K.: Seismic damage analys is of rein forced concrete buildings. Structure Engineering, 111(4):740-757, 1985.

Qu, Y., Yue, Q., Bi, X. and Kärnä, T.: A random ice force model for narrow conical structures. Cold Regions Science and Technology, 45(3), 148-157, 2006.

20   RIL, RIL-144, (2001), Finnish civil engineers association, Guideline for the loading of structures

SANDERSON T.: Ice Mechanics: Risks to Offshore Structures. London: Graham & Trotman,1988.

Sanderson, T.: Ice Mechanics: Risks to Offshore Structures, London: Graham & Trotman, 1988.

Singhal, A. and Kiremidjian, A.S.: Method for probabilistic evaluation of seismic structural damage, Journal of Structural Engineering, 122(12), 1459-1467, 1996.

25   SOAPRC.: Statistical communique of maritime hazard of China from 2001–2016, State Oceanic Administration, People's Republic of China, 2017.

Sparks, P.R., Schiff, S.D. and Reinhold, T.A.: Wind damage to envelopes of houses and consequent insurance losses. Journal of Wind Engineering & Industrial Aerodynamics, 53(1–2), 145-155, 1994.

State Oceanic Administration.: Technical Guidelines for Risk Assessment and Zoning of Sea Ice Disasters, 2016.

30   Su, H. and Wang, Y.: Monitoring the spatiotemporal evolution of sea ice in the bohai sea in the 2009–2010 winter combining modis and meteorological data. Estuaries and Coasts, 35(1), 281-291, 2012

Tachiiri, K.: Quantitative risk assessment for future meteorological disasters. Climatic Change, 113(3-4), 867-882, 2012.

Timco, G. W., Irani, M. B., Tseng, J., Liu, L. K., and Zheng, C. B.: Model tests of dynamic ice loading on the chinese jz-20-2 jacket platf. Canadian Journal of Civil Engineering, 19(5), 819-832, 2011.

Wang, F., Zou, Z. J., Zhou, L., Ren, Y. Z. and Wang, S. Q.: A simulation study on the interaction between sloping marine structure and level ice based on cohesive element model. Cold Regions Science and Technology, 149, 2018.

5 Wang, X. Y., Yuan, B. K. , Shang, J. and Li G.: Disaster of sea ice and defence Countermeasures in the Bohai Sea and the Yellow Sea, Coastal Engineering, 30(4), 46-55, 2011.

Wang, Y., Yue, Q., Guo, F., Bi, X., Shi, Z. and Yan, Q.: Performance evaluation of a new ice-resistant jacket platform based on field monitoring. Cold Regions Science and Technology, 71(1), 44-53, 2012.

Yue, Q. J., Qu, Y., Bi, X. J., and Karna, T.: Ice force spectrum on narrow conical structures. Cold Regions Science and

10 Technology, 49(2), 161-169, 2007a.

Yue, Q. J., Yuan, L., Zhang, R. X., Yan, Q. U. and Wang, R. X.: Ice-induced fatigue analysis by spectral approach for offshore jacket platforms with ice-breaking cones. China Ocean Engineering, 21(1), 1-10, 2007b.

Yue, Q. J., Zhang, D. Y., Liu, Y. and Tong, B. L.: Failure modes analysis of ice-resistant compliant structures based on monitoring oil platforms in Bohai Gulf. Ocean Engineering, 26(1), 18-23, 2008

15 Yue, Q., Guo, F., and Karna, T.: Dynamic ice forces of slender vertical structures due to ice crushing. Cold Regions Science & Technology, 56(2), 77-83, 2009.

Zhang, D. Y., Yue, Q. J., Che, X. F., Liu, Y. and Li, H. H.: Dynamic characteristics analysis of ice-resistant jacket platforms in Bohai Sea. Ocean Engineering, 28(1), 18-24, 2010.

Zhang, D., Wang, G., Yue, Q. and Lou, C.: Structural Ice-resistant Performance Evaluation of Offshore Wind Turbine

20 Foundation, Proceedings of the 26th International Ocean and Polar Engineering Conference, 26 June-2 July, 16TPC-0778, 2016.

Zhang, D., Xu, N., Yue, Q., and Liu, D: Sea ice problems in bohai bay oil and gas exploitation. Journal of Coastal Research, 73, 676-680, 2015.

Zhang, H., Li, J., Yin, L., Zhang, T., Ning, L. and Zhang, Q.: Risk quantitative technology of oil and gas drilling engineering.

25 Journal of Safety Science and Technology, 8(8), 127-131, 2012.

Zhang, J. Q. and Li, N.: Quantitative methods and applications of risk assessment and management on main meteorological disasters, Beijing Normal University press, 2007.

Zhang, X. L., Zhang, Z. H. and Zong J.: Sea ice disasters and their impacts since 2000 in Laizhou Bay of Bohai Sea, China. Natural Hazards, 65(1), 27-40, 2013.

30 Zhao, Q., Liu, Y., Tang, M. N. and Shi, J. P.: Numerical sea ice forecast for the Bohai Sea in the winter of 2012-2013, Marine Forecasts, 31(2), 73-79, 2014.